


From Non-Detection to Detection: Atacama Compact Array Mosaic Observations of Faint Extended [C I] Emission in NGC 7679

TOMONARI MICHİYAMA ¹, TOSHIKI SAITO,² KOUICHIRO NAKANISHI,^{3,4} DAISUKE IONO,^{3,4} KEN-ICHI TADAKI,⁵ JUAN MOLINA,⁶ BUMHYUN LEE,^{7,8} MING-YANG ZHUANG,⁹ JUNKO UEDA,³ TAKUMA IZUMI,^{3,4} AND LUIS C. HO^{10,11}

¹*Faculty of Information Science, Shunan University, 843-4-2 Gakuendai, Shunan, Yamaguchi, 745-8566, Japan*

²*Faculty of Global Interdisciplinary Science and Innovation, Shizuoka University, 836 Ohya, Suruga-ku, Shizuoka 422-8529, Japan*

³*National Astronomical Observatory of Japan, National Institutes of Natural Sciences, 2-21-1 Osawa, Mitaka, Tokyo, 181-8588, Japan*

⁴*Department of Astronomical Science, The Graduate University for Advanced Studies, SOKENDAI, 2-21-1 Osawa, Mitaka, Tokyo, 181-8588, Japan*

⁵*Faculty of Engineering, Hokkai-Gakuen University, Toyohira-ku, Sapporo 062-8605, Japan*

⁶*Instituto de Física y Astronomía, Universidad de Valparaíso, Avda. Gran Bretaña 1111, Valparaíso, Chile*

⁷*Department of Astronomy, Yonsei University, 50 Yonsei-ro, Seodaemun-gu, Seoul 03722, Republic of Korea*

⁸*Korea Astronomy and Space Science Institute, 776 Daedeokdae-ro, Daejeon 34055, Republic of Korea*

⁹*Astronomy Department, University of Illinois Urbana-Champaign, Urbana, IL 61801, USA*

¹⁰*Kavli Institute for Astronomy and Astrophysics, Peking University, 5 Yiheyuan Road, Haidian District, Beijing 100871, P.R.China*

¹¹*Department of Astronomy, School of Physics, Peking University, Beijing 100871, China*

ABSTRACT

We report the detection of [C I] $^3P_1-^3P_0$ emission in the nearby galaxy NGC 7679 using the Atacama Compact Array (ACA) of the Atacama Large Millimeter/submillimeter Array (ALMA). In Michiyama et al. (2021), [C I] $^3P_1-^3P_0$ emission in NGC 7679 was reported as undetected based on ACA observations conducted in 2019 (ALMA Cycle 6). These observations had ~ 1 minute on-source time and used a single pointing with a field of view (FoV) of $\sim 20''$. In 2023 (Cycle 9), we carried out mosaic observations using seven pointings with an FoV of $\sim 27''$ and 4–5 minutes on-source per pointing. The additional data have significantly improved the line sensitivity, uv -sampling, and noise uniformity across the galaxy disk. Our Cycle 9 observations confirm the presence of extended [C I] $^3P_1-^3P_0$ emissions in NGC 7679, which was completely missed in the Cycle 6 observations due to insufficient sensitivity and uv -sampling. This highlights the basic technical challenges of estimating the total flux by interferometric observations with sparse uv sampling.

Keywords: Extragalactic astronomy (506) — Submillimeter astronomy (1647) — Interstellar medium (847)

1. INTRODUCTION

The lower forbidden 3P fine structure transition of atomic carbon, denoted as [C I] $^3P_1-^3P_0$ or [C I] (1–0), emits at a rest frequency of 492 GHz ($\lambda = 609 \mu\text{m}$). Michiyama et al. (2021) conducted a survey project observing the [C I] (1–0) and CO (4–3) emission in nearby ultra/luminous infrared galaxies (U/LIRGs) during the Atacama Large Millimeter/submillimeter Array (ALMA) Cycle 6 period using the 7-m array of

the Atacama Compact Array (ACA), without the total power (TP) array. This effort identified three galaxies: NGC 6052 (Michiyama et al. 2020), NGC 7679, and ESO 467-G027, showing notably faint [C I] (1–0) emissions compared to that of CO (4–3). In this report, we present the detection of [C I] (1–0) toward NGC 7679 and briefly discuss the difficulties we faced.

2. DATA

2.1. Observations

The target, NGC 7679, is a nearby galaxy with a redshift of $z = 0.0171$. The observing frequency for redshifted [C I] (1–0) is 483.887 GHz. The ACA observations targeting [C I] (1–0) emission in NGC 7679 were

performed during the Cycle 9 season (ALMA project ID: 2022.1.00746.S; PI: T. Michiyama). On June 15, 2023, mosaic observations (seven pointings) using the 7-m array were conducted, with an on-source time of about 4–5 minutes per pointing. This on-source time is longer than that in the previous Cycle 6 observation, which was ~ 1 minute. The TP array observations were conducted on October 13, 2022, and April 13, 2023.

2.2. Data Reduction

The calibrated visibility data were obtained by running the standard pipeline calibration scripts provided by ALMA using CASA (CASA Team et al. 2022). The imaging processes were conducted using CASA 6.5.0-15, with a velocity resolution of 30 km s^{-1} , a cell size of $0''.25$, an imaging size of 256 pixels, and Briggs weighting with a robust parameter of 0.5. The clean masks for each channel were manually determined. We performed the same clean task in both Cycle 6 (single-point) with a FoV of $\sim 20''$ and Cycle 9 (7-pointing mosaic) with a FoV of $\sim 27''$. For a fair comparison, we used the same maximum and minimum baselines ($[14, 69] \text{ k}\lambda$) in both datasets (see the top panel of Figure 1), and the synthesized beam was smoothed to $3''.5$. The rms noise level of the data cube was $\sim 0.02 \text{ Jy beam}^{-1}$ in the Cycle 9 data and $\sim 0.08 \text{ Jy beam}^{-1}$ in the Cycle 6 data. The moment 0 map was made by integrating the channels of $[-150, 150] \text{ km s}^{-1}$ without applying any masking.

2.3. Results

The velocity integrated intensity (moment 0) map of the Cycle 9 data clearly shows the detection of the [C I] (1–0) emission line (see the middle panel of Figure 1). We measure an integrated flux of $123 \pm 10 \text{ Jy km s}^{-1}$ by applying a two-dimensional Gaussian fit to sources in the moment 0 image using the `imfit` task in CASA. It is important to note that this integrated flux might not represent the “total” [C I] (1–0), as the line flux of the tentatively detected [CI] by the TP array (Michiyama et al. in prep.) may be further higher than what we measured with the ACA here.

3. DISCUSSION

Because the sensitivity in the Cycle 9 observations is four times better than that in Cycle 6, the new detection is reasonable. When we create an image using a single scan for the central pointing in the Cycle 9 dataset, we detect no emission consistent with the Cycle 6 observation. The bottom panel of Figure 1 highlights that the source remains undetected, even when simply summing the values of each pixel in the channel map. For instance, in the case of a smaller aperture ($5''$ circle shown

by the blue line in the bottom panel of Figure 1), the spectrum in the Cycle 6 data appears similar to that in the Cycle 9 data around the line detection frequency range. However, when integrating the spectrum over the pixels within a larger aperture, the Cycle 9 spectrum shape is not reproduced.

A concern arises from the contradiction between the upper limit derived from the Cycle 6 moment-0 map and the integrated flux calculated from the Cycle 9 data. This is due to a fundamental weakness when dealing with spatially extended sources. As shown in equation (4) of Michiyama et al. (2021), an emission line flux upper limit can be estimated as:

$$S_{\text{line}}\Delta v < 3\sigma_{\text{ch}}\Delta V_{\text{ch}}\sqrt{\frac{N_{\text{ch}}N_{\text{S}}}{N_{\text{B}}}}, \quad (1)$$

where σ_{ch} is the RMS noise level in the channel map, ΔV_{ch} is the velocity resolution, $N_{\text{ch}} = \text{FWHM}/\Delta V_{\text{ch}}$ is the number of channels within the FWHM, N_{S} is the number of pixels corresponding to the source size, and N_{B} is the number of pixels within the synthesized beam. If the source distribution is unknown, assumptions must be made regarding the line profile and source size. For example, assuming $\text{FWHM} = 150 \text{ km s}^{-1}$ and $N_{\text{S}}/N_{\text{B}} = 3$, the 3σ upper limit is calculated as $S_{\text{line}}\Delta v < 30 \text{ Jy km s}^{-1}$ for $\Delta V_{\text{ch}} = 30 \text{ km s}^{-1}$ and $\sigma_{\text{ch}} = 0.08 \text{ Jy beam}^{-1}$, based on our Cycle 6 data. This upper limit is inconsistent with the integrated flux measured in Cycle 9 data. However, the equation (1) assumes that the [C I] ${}^3P_1-{}^3P_0$ emission exhibits a spatial distribution detectable within the limited uv -sampling and FoV of a single-pointing observation, as in Cycle 6. If the emission is spatially extended, it is not surprising that the flux detected in Cycle 9 was completely missed in Cycle 6. The new detection can be attributed to the longer integration time and mosaicking in Cycle 9, which improved the uv -coverage and ensured uniform noise across the entire map (Figure 1).

As CO (4–3) observations were not conducted in Cycle 9, the new detection of [C I](1–0) does not fully negate the conclusions of a low [C I] (1–0)/CO (4–3) ratio reported by Michiyama et al. (2021). This is because CO (4–3) observations from Cycle 6 may have also missed the diffuse components. Finally, we note that Michiyama et al. (2020) reported a non-detection of the [C I] (1–0) line in the nearby galaxy NGC 6052, which was observed in the same survey project as NGC 7679 in Cycle 6. Since the new ACA observations of NGC 6052 assigned in Cycle 9 were not completed, we cannot determine whether the faintness of the [C I] (1–0) line in NGC 6052 is real or not at this stage.

We thank Dr. Ran Wang for her valuable discussions. T.M. was supported by a University Research Support Grant from the National Astronomical Observatory of Japan (NAOJ). T.S. was supported by the Daiichi-Sankyo “Habataku” Support Program for the Next Generation of Researchers. K.N. acknowledges support from the JSPS KAKENHI grant No. 19K03937. This report makes use of the following ALMA data: ADS/JAO.ALMA 2022.1.00746.S and 2018.1.00994.S.

Facilities: ALMA

Software: ALMA Calibration Pipeline and CASA

REFERENCES

- CASA Team, Bean, B., Bhatnagar, S., et al. 2022, PASP, 134, 114501, doi: [10.1088/1538-3873/ac9642](https://doi.org/10.1088/1538-3873/ac9642)
- Michiyama, T., Ueda, J., Tadaki, K.-i., et al. 2020, ApJL, 897, L19, doi: [10.3847/2041-8213/ab9d28](https://doi.org/10.3847/2041-8213/ab9d28)
- Michiyama, T., Saito, T., Tadaki, K.-i., et al. 2021, ApJS, 257, 28, doi: [10.3847/1538-4365/ac16df](https://doi.org/10.3847/1538-4365/ac16df)

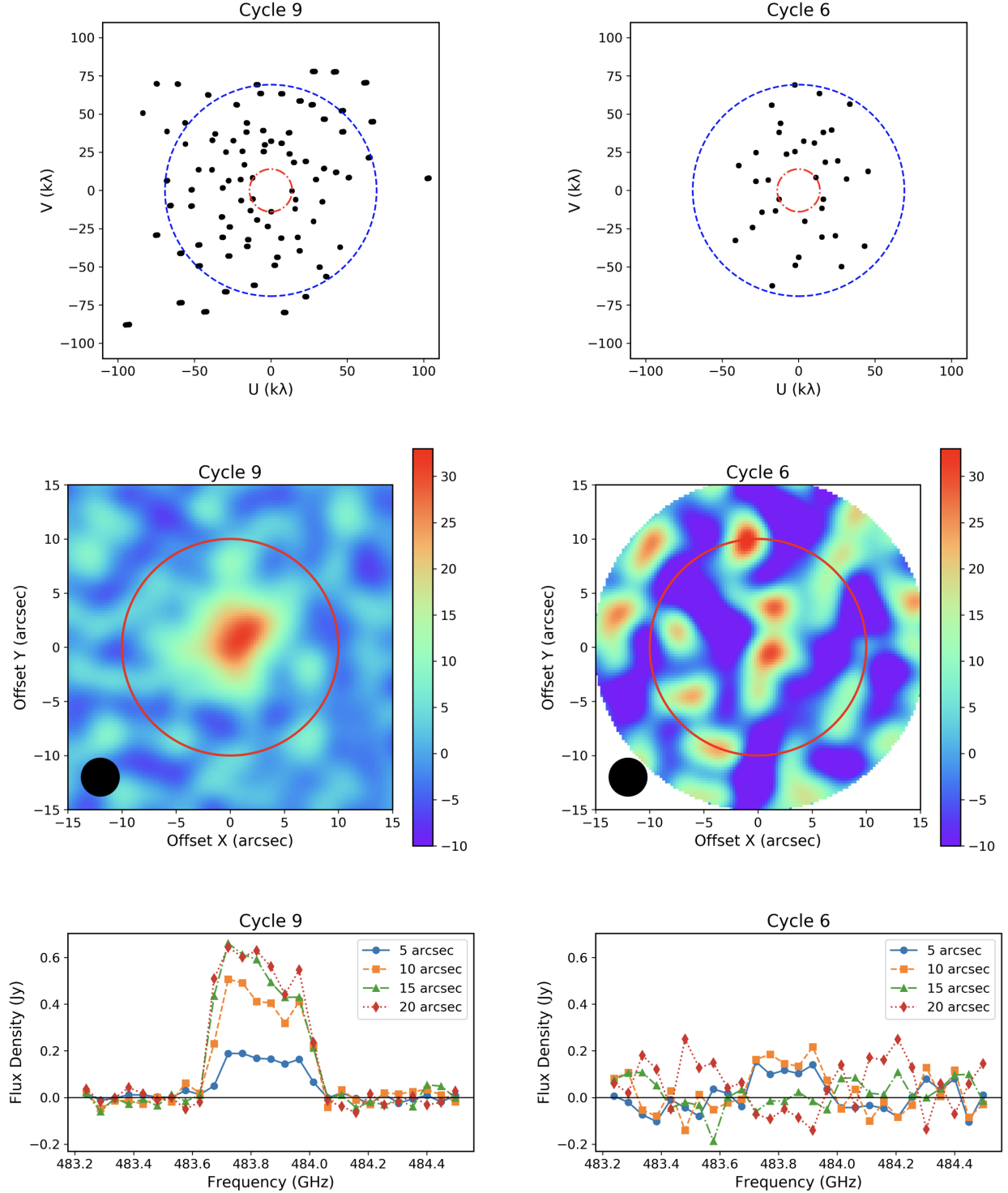


Figure 1. The results of ACA observation targeting [C I] (1–0) emission in NGC 7679. The comparison between Cycle 9 (left) and Cycle 6 (right). (Top:) The visibility distribution on the uv -plane. The blue and red dots represent the maximum and minimum uv distances corresponding to baseline lengths in Cycle 6. (Middle:) The moment 0 map with the color scale of $[-10, 33] \text{ Jy km s}^{-1} \text{ beam}^{-1}$. The red line indicates a circle with a diameter of 20 arcseconds. The black-filled circle indicates the synthesized beam of $3''.5$. (Bottom:) The lines indicate the spectra obtained with different apertures of 5 (blue), 10 (orange), 15 (green), and 20 (red) arcseconds. The black line represents the zero level.